

Supporting Information for “Stabilizing effect of compositional viscosity contrasts on thermochemical piles”

Björn H. Heyn¹, Clinton P. Conrad¹, Reidar G. Trønnes^{1,2}

¹Centre for Earth Evolution and Dynamics (CEED), University of Oslo, Norway

²Natural History Museum, University of Oslo, Norway

Contents

1. Text S1 to S2
2. Figure S1 to S2
3. Tables S1 to S2

Introduction

This supporting information provides a discussion about the chosen model resolution, the imposed degree-2 structure and tables with all parameters characterizing the geodynamical models discussed in the paper.

Text S1.

In order to ensure that our models capture the dynamics of entrainment, we performed resolution tests with three different meshes:

1. 45 nodes in radial and 157 nodes in longitudinal direction, uniform mesh (LR-models)
2. 69 nodes in radial and 237 nodes in longitudinal direction, radially refined in the lowermost 809 km (MHR-models)
3. 91 nodes in radial and 313 nodes in longitudinal direction, radially refined in the lowermost 809 km (VHR-models, used in the main document).

The resolution at the CMB (radial x horizontal) is approximately 65 km x 35 km for LR, 21 km x 23 km for MHR and 17 km x 17 km for VHR. We compared our models using a thermal viscosity contrast of $\eta_{\Delta T} = 65$ by mapping the contours of 20%, 50% and 80% remaining pile mass. The results are shown in Figure S1a-c. As can be seen, more combinations of the buoyancy number B and the compositional viscosity contrast η_C result in piles with more than 80% mass if the resolution is increased. This holds true for the other contour lines as well. However, the lines get flatter in the η_C - B -space, indicating a reduced importance of the excess density while the viscosity remains a controlling factor.

We also performed a few additional tests with even higher resolution (UHR-models, 139 by 481 nodes, thus 10 km x 11 km) for $B = 0.7$, $\eta_{\Delta T} = 65$ and two different compositional viscosity contrasts of $\eta_C = 10$ (case 1) and $\eta_C = 4$ (case 2). The resulting piles have almost the same mass as for the VHR-cases, the differences being $\sim 1\%$ for the stable pile with $\eta_C = 10$ and $\sim 11\%$ for the unstable and time-dependent case of $\eta_C = 4$. The pile masses retained after 4.5 Gyrs for case 1 with different resolutions (LR, MHR, VHR, and UHR) are compared in Figure S1d. While both LR- and MHR-models result in piles with about 20% remaining mass, VHR- and UHR-models produce piles with $> 80\%$ mass and only minor differences. This confirms that our VHR-models are able to capture the evolution of the pile mass qualitatively well enough for our purpose. Minor adjustments of the contour

Corresponding author: Björn H. Heyn, b.h.hey@geo.uio.no

lines for 20%, 50% and 80% might be expected for resolutions < 10 km, but they should not affect our general conclusions.

Apart from the resolution, the shape of the chosen elements affects the observed entrainment of the dense material. A few tests with a resolution of 45 by 313 nodes (34 x 17 km at the CMB) and mesh refinement in the lowermost mantle show increased entrainment compared to LR-models, although the higher resolution would suggest the oppsite. However, elements stretched in radial direction significantly overestimate entrainment, even overcompensating the effect of increased resolution. As a consequence, we chose cubic-shaped elements and avoided elongated elements.

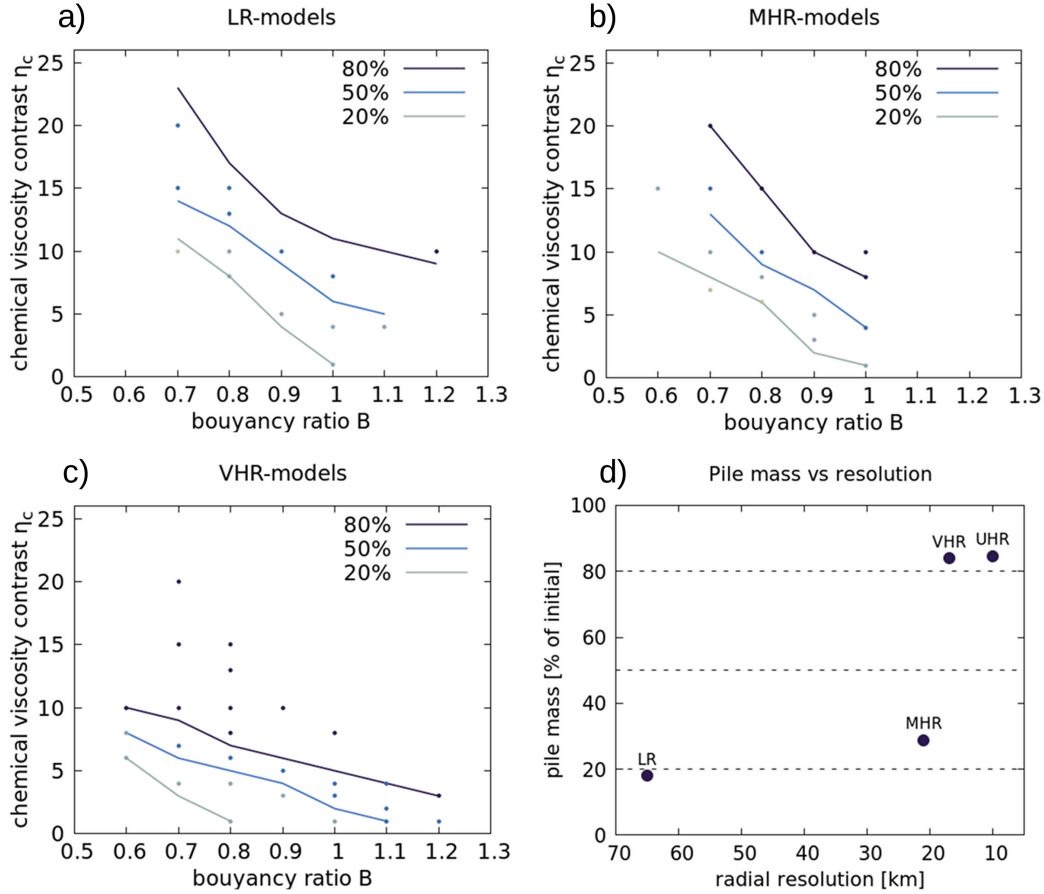


Figure S1. (a)-(c) Contour lines of 20%, 50% and 80% remaining pile mass after 4.5 Gyrs for models with different resolution: (a) LH-models, (b) MHR-models and (c) VHR-models as used in the main text. The thermal viscosity contrast is fixed to $\eta_{\Delta T} = 65$. The general trend of a trade-off between η_C and B is not affected by the resolution, although the necessary η_C value for a given contour decreases with higher resolution. (d) Comparison of obtained pile masses for $B = 0.7$, $\eta_{\Delta T} = 65$ and $\eta_C = 10$ after 4.5 Gyrs with LR-, MHR-, VHR- and UHR-models. Piles for both LR- and MHR-models are in the unstable regime with time-dependent mass, while VHR- and UHR-models result in stable piles of the same mass.

Text S2.

To test the affect of the imposed degree-2 pattern on our results, we examined models in which we reversed the plate velocity after succesful formation of the piles. More specifically, we developed piles using models with $B = 1.2$, $\eta_C = 10$ and $\eta_{\Delta T} = 2.3$ after 5.0 Gyrs. We then reversed the plate velocities and forced subduction on top of the pile. An example of 3 snapshots during the temporal evolution of the pile for $B = 0.7$, $\eta_C = 7$ and $\eta_{\Delta T} = 65$ is shown in Figure S2. As can be seen, the pile is initially pushed away from its original position (Figure S2a), gets trapped between the old and the new slab (Figure S2b) until the remaining slab material is heated up sufficiently and finally the pile gets pushed to the opposite boundary (Figure S2c). During this process, the dense material gets deformed and entrainment increases, but remains smaller than during the initial overturn preceding pile formation.

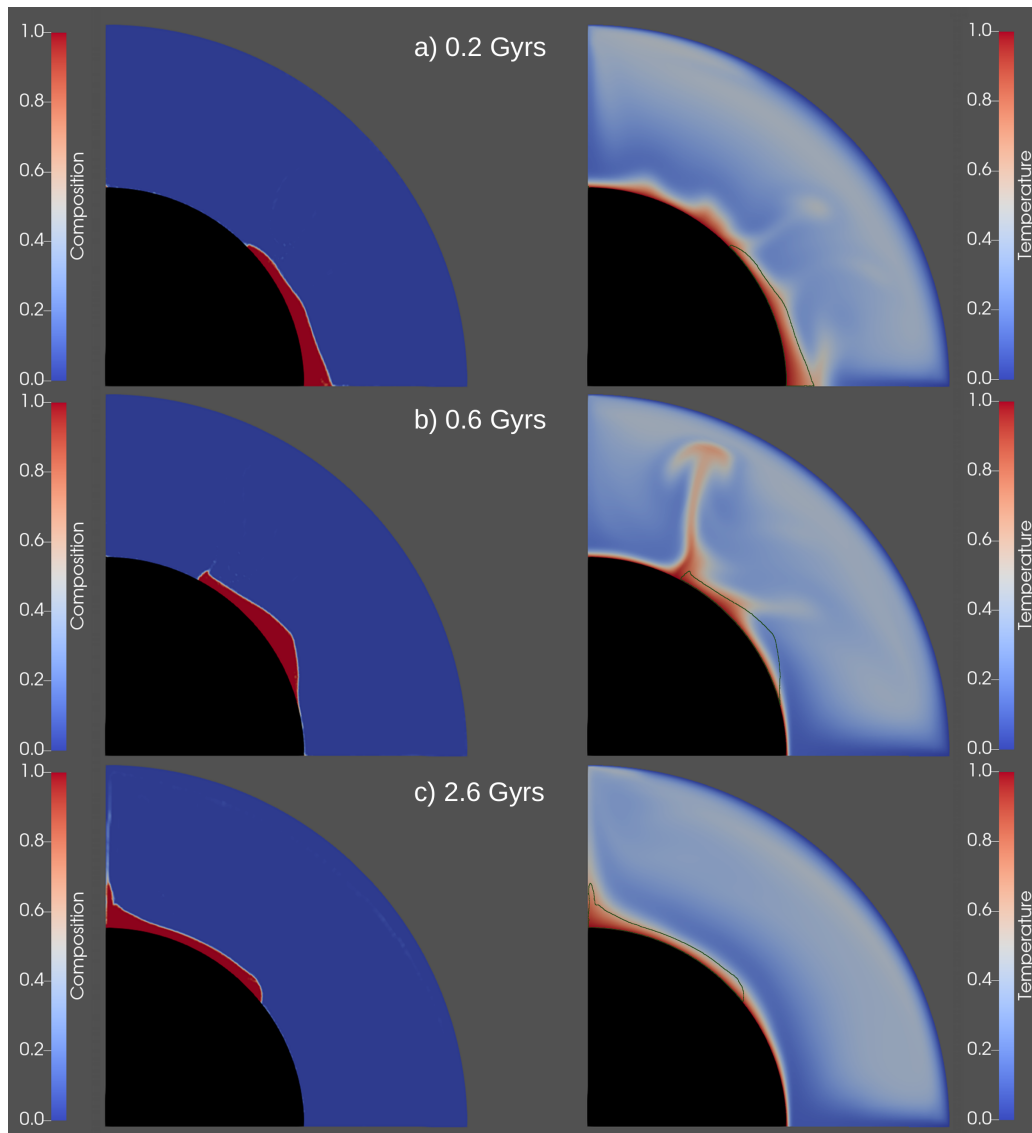


Figure S2. Examples of the temporal evolution for $B = 0.7$, $\eta_C = 7$ and $\eta_{\Delta T} = 65$ for a case in which the imposed surface velocity is reversed after pile formation is completed. (a), (b) and (c) show the compositional field (left) and the corresponding temperature fields (right) for timesteps 0.2 Gyrs, 0.6 Gyrs and 2.6 Gyrs after velocity reversal. Dark lines in the temperature fields indicate the pile shapes for $cl = 0.8$.

Table S1. Characteristic parameters for thermochemical calculations. Non-dimensional values are converted according to the scaling laws given in the CitcomS manual^a. For the conversion of B , we assume a temperature drop across the mantle of 3200 K and a thermal expansivity of $\alpha = 1 \cdot 10^{-5}$ at the CMB [Tackley, 2012]; values give the chemical excess density of the pile material in percent relative to the reference density. Ra is set to 10^8 , which results in an effective Rayleigh number of about 10^7 due to the use of the Earth's radius R_0 instead of the mantle thickness d in the definition of Ra .

Parameter	Symbol	Non-dimensional Value	value [Unit]
Gravitational acceleration	g		9.81 [m/s ²]
Mantle thickness	d	0.45	2891 [km]
Reference density	ρ		$3.34 \cdot 10^3$ [kg/m ³]
Reference viscosity	η	1.0	$1.0 \cdot 10^{21}$ [Pa s]
Thermal diffusivity	κ		$1.0 \cdot 10^{-6}$ [m ² /s]
Thermal expansivity	α		$3.0 \cdot 10^{-5}$ [1/K]
Buoyancy ratio/ chemical excess density	B	0.4-1.2	1.28%-3.84%
Rayleigh number	$Ra = \frac{\alpha \rho g \Delta T d^3}{\eta \kappa}$	10^7	
Internal heating rate	H	10	$2.96 \cdot 10^{-16}$ [W/kg]
Initial thickness of dense layer	d	0.02	127 [km]
Imposed surface velocity	v_{surf}	3000	1.48 [cm/yr]
Compositional viscosity contrast	η_C	1-20	
Thermal viscosity contrast	$\eta_{\Delta T}$	2.3– 330	

^aCitcomS User Manual Version 3.3.0, CIG, www.geodynamics.org.

Table S2. Parameters defining the viscosity profiles according to the thermal viscosity contrast $\eta_{\Delta T}$. Steps for the activation energy E_η , the temperature offset T_η and the viscosity prefactor η_0 are set at non-dimensional depths of 0.047, 0.064 and 0.104, which scale to 299 km, 410 km and 660 km, respectively. Values are sorted by increasing depth.

$\eta_{\Delta T}$	η_0	E_η	T_η
2.3	5 / 0.5 / 2.5 / 10	1 / 1 / 1 / 1	0.02 / 0.4 / 0.6 / 0.7
65	5 / 0.5 / 2.5 / 10	1 / 1 / 1 / 1	0.02 / 0.2 / 0.2 / 0.2
330	5 / 0.5 / 2.5 / 5	1 / 1 / 1 / 1	0.02 / 0.15 / 0.15 / 0.15
1700	5 / 0.5 / 2.5 / 5	1 / 1 / 1 / 1	0.02 / 0.12 / 0.12 / 0.12
7500	5 / 0.5 / 2.5 / 5	1.2 / 1.2 / 1.2 / 1.2	0.02 / 0.12 / 0.12 / 0.12